



HAL
open science

Hetero-Bimetallic Effect as a Route to Access Multinuclear Complexes

Zhongrui Chen, Gabriel Canard, Denis Jacquemin, Christophe Bucher, Michel Giorgi, Olivier Siri

► **To cite this version:**

Zhongrui Chen, Gabriel Canard, Denis Jacquemin, Christophe Bucher, Michel Giorgi, et al.. Hetero-Bimetallic Effect as a Route to Access Multinuclear Complexes. *Inorganic Chemistry*, 2018, 57 (20), pp.12536-12542. 10.1021/acs.inorgchem.8b01466 . hal-01891114

HAL Id: hal-01891114

<https://hal.science/hal-01891114>

Submitted on 31 Jan 2020

HAL is a multi-disciplinary open access archive for the deposit and dissemination of scientific research documents, whether they are published or not. The documents may come from teaching and research institutions in France or abroad, or from public or private research centers.

L'archive ouverte pluridisciplinaire **HAL**, est destinée au dépôt et à la diffusion de documents scientifiques de niveau recherche, publiés ou non, émanant des établissements d'enseignement et de recherche français ou étrangers, des laboratoires publics ou privés.

Heterobimetallic effect as a new route to access multinuclear complexes

Zhongrui Chen,[†] Gabriel Canard,[†] Denis Jacquemin,^{*‡} Christophe Bucher,[§] Michel Giorgi[⊥] and Olivier Siri^{*†}

[†] Aix Marseille Université, CNRS UMR 7325, CINaM, Campus de Luminy, case 913, 13288 Marseille cedex 09 (France)

[‡] CEISAM UMR CNRS 6230, Université de Nantes, 2 rue de la Houssinière, BP 92208, 44322 Nantes Cedex 3 (France)

[§] Laboratoire de Chimie UMR 5182, CNRS – Univ. Lyon, ENS de Lyon, Univ. Claude Bernard Lyon 1, Lyon (France)

[⊥] Aix Marseille Univ, CNRS, Centrale Marseille, FSCM, Marseille (France)

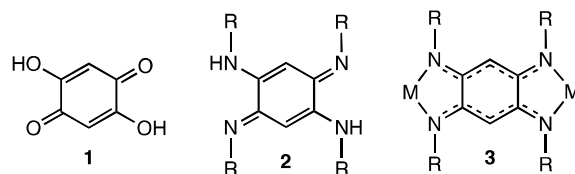
ABSTRACT: We report the synthesis of a key mononuclear intermediate complex based on a quinoid ligand, and its further metalation to afford the corresponding heterobimetallic compound that revealed unique properties. An unprecedented heterobimetallic effect in coordination chemistry could be indeed observed and exploited to prepare, through selective ligand exchange, a tetranuclear complex (Pd-Ni-Ni-Pd) absorbing light up to the far-red region. Most importantly, we describe here to the best of our knowledge the first use of bischelating ligand for ligand exchange and this approach can be considered as a new route for incorporating planar units to access multi-heteronuclear complexes. The origin of this specific ligand exchange as well as of the nature of the electronic excited-states of the relevant structures have been investigated by first-principle calculations.

INTRODUCTION

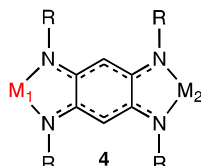
Quinones belong to one of the most important classes of π -conjugated molecules with applications covering a broad spectrum ranging from chemistry to materials science, physics to biology, and engineering to medicine.¹ Quinones have attracted considerable interest in coordination chemistry because their π^* -orbitals can mix extensively with the valence d-orbitals of a metal center, allowing a full electron delocalization over both metal and ligand.² As a consequence, remarkable properties emerged especially for complexes based on bis-chelating quinoidal ligands which could be used in catalysis, molecular electronics, magnetism or optics.³ The classical bis-chelating ligand in quinoid chemistry is the widely used 2,5-dihydroxy-1,4-benzoquinone **1** that can bind one, two or more metal centers.⁴ Noteworthy, although **1** is probably the most used quinoid ligand (more than 200 complexes have been reported), there are currently no record on heteronuclear complexes, most probably due to the high reactivity of both chelating sites.

The nitrogenated analogues **2** are in the limelight of coordination chemistry because of (i) the presence of N-substituents that can be tuned almost at will⁵, and (ii) the easy introduction of metal centers to form mono-⁶ and dinuclear complexes.³ These latter compounds (**3**) have been shown to be particularly useful in magnetism (M = Cu, Fe, Cr, Mn, Co),⁷ catalysis (M = Ni),⁸ polymer (M = Na),⁹ electromism (M = Pt)¹⁰ and optics (M = Ir).¹¹ The great potential of homodinuclear complexes (**3**) led us to investigate strategies which could provide access to the as yet unknown heterometallic analogues **4**, featuring two different metal centers. We reasoned that the persistent failure to access such heterobimetallic species could arise from the poor stability of the mononuclear complexes reported so far. To address this issue, we propose here a stepwise approach based on the synthesis of square planar d⁸ metal mononuclear complexes enabling to maximize the electronic delocalization over the whole molecule, and consequently their stability.

Previously



This work



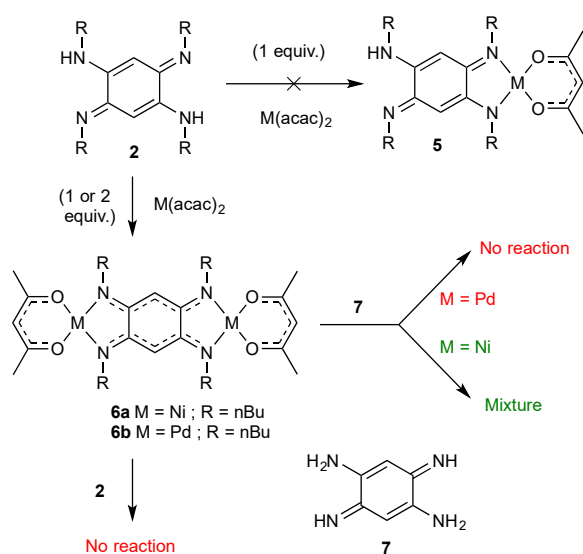
As a preliminary step, we have focused on strategies allowing to produce multinuclear complexes by selective ligand exchanges since these reactions are metal-dependent and favored or unfavored depending on the affinity of the ligand. Interestingly, ligand substitutions in planar nickel(II) complexes have been extensively investigated for monodentate ligands,¹² but never with bischelating motifs such as **2**.

In the present work, we report three major advances in coordination chemistry: (i) the synthesis of an unknown square planar mononuclear complex based on N_4 -type ligand **2**, (ii) the complexation of two different metal center to afford the first heterobimetallic complex in quinonediimine chemistry, and (iii) a remarkable heterobimetallic effect that could be exploited to achieve a regioselective synthesis of coordination oligomers, one metal center being used as a reactive site (Ni) while the second one only plays the role of stopper (Pd). This latter process involves the incorporation, through selective exchange, of an exogenic ditopic binding moieties to yield a multinuclear complex (Pd-Ni-Ni-Pd) that presents a pronounced far-red absorption. Such straightforward exchange reactions have thus been implemented to achieve control over the length of metal-ligand oligomers involving the quinoid ligand **2**. The electronic effects of the metal ligation and the ligand exchange have been investigated by absorption spectroscopy and rationalized by *ab initio* calculations.

RESULTS AND DISCUSSION

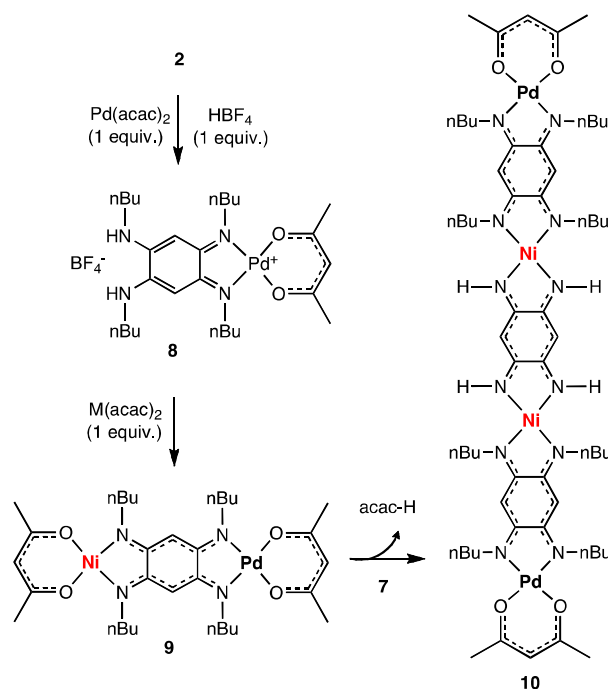
The synthesis of square planar mononuclear complexes was first envisaged by reacting a stoichiometric amount of ligand **2** ($R = nBu$) and $M(acac)_2$ (in THF for $M = Ni$ or dioxane for $M = Pd$). Unfortunately, this reaction did not afford the expected complex **5** but the dinuclear species **6a** and **6b** (Scheme 1). Selective formation of these complexes can be explained by an allosteric effect implying that metalation of the first chelating site enhances the metal-binding ability of the second site. In other words, **5** can be seen as an “activated” intermediate featuring improved metal-binding properties. The homodinuclear species **6a** and **6b** could be obtained in much better yields (72 and 70% respectively) from **2** when using two molar equivalents of $M(acac)_2$. Their stability could be established both at the solid-state and in solution, even in the presence of an excess of **2** (Scheme 1).

Scheme 1. Synthesis and reactivity of homodinuclear complexes **6a-b**



Remarkably, introduction of unsubstituted ligand **7** to a solution of **6a** and **6b** (up to 70°C) revealed a drastic difference in reactivity depending on the metal centers. If an inseparable mixture of oligomers could be observed from **6a** (M = Ni), no reaction could be observed upon the same conditions from **6b**, evidencing both the crucial role of the metal and the impact of using an unhindered ligand **7** instead of **2**. This observation can be explained by ligand substitution often encountered on planar nickel(II) complexes that undergo exchange ligand reactions.¹³ These results prompted us to devise synthetic strategies providing access to the heterobinuclear analogue **9** wherein: (i) the Ni(II) site could be available for ligand exchange, and (ii) the Pd(II) center could behave as a « stopper » preventing the formation of oligomers on this side. To address the above-mentioned allosteric effect, the metalation reaction was conducted in the presence of an acid used to annihilate the reactivity of the « metal free » binding site by selective protonation of one nitrogen atom. Thus, the free ligand **2** (R=*n*-Bu) was thus reacted with 1 equiv. of Pd(acac)₂ and 1 molar equiv. of HBF₄ in 1,4-dioxane to afford the corresponding mononuclear complex **8** as a dark powder in 81% yield (Scheme 2).

Scheme 2. Stepwise synthesis of mono- (8), heterodi- (9) and heterotetranuclear (10) complexes



X-ray diffraction analysis of complex **8** indicates the mono-metallation of the ligand and the presence of BF₄ anion to balance the monocationic charge on the palladium center (see Figure 1 for **8**). Close examination of the bond distances within the N(1)-C(1)-C(2)-C(3)-N(3) and N(4)-C(4)-C(5)-C(6)-N(2) moieties of **8** revealed an alternating succession of single and double bonds and the presence of two imine functions in *ortho* position [C(1)-N(1) and C(6)-N(2)], whereas the C(1)-C(6) and C(3)-C(4) are single bonds with respective distances of 1.502(4) and 1.493(4) Å, highlighting the lack of conjugation between the two halves of the molecule. These data thus reveal that coordination of a metal center comes along with a *para*→*ortho* isomerization of the ligand⁶ which provides a square planar environment around the metal center, hitherto unknown for mononuclear complexes based on **2**.

Next, **8** was reacted with an excess of Ni(acac)₂ in MeOH at 60 °C. The obtained precipitate was isolated by filtration to afford a brown powder identified as being the targeted heteronuclear complex **9** (37% yield). In contrast to **8**, X-ray diffraction study on single crystals of **9** revealed an extensive π-electronic delocalization (uniform bond lengths over the whole structure) whereas the lack of significant conjugation between the two 6π-subsystems was maintained, as already observed for homobimetallic complexes such as **6a** and **6b** and related dinickel complexes.⁸ The presence of the two different metals (Ni and Pd) was clearly established (by comparison with the X-ray data of **6a** and **6b**, see SI), the metal centers and the ligand being *quasi* in the same molecular plane.

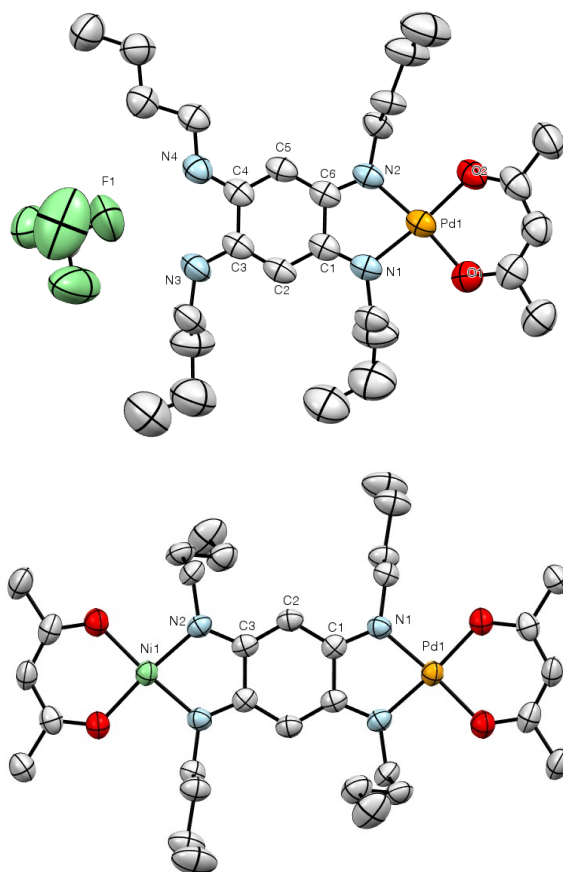


Figure 1. ORTEP views of **8** and **9** (H atoms are omitted for clarity).

Interestingly, comparative NMR studies carried out on **6a**, **6b** and **9** revealed that the heterobimetallic complex (**9**) exhibits key distinctive features of both homobimetallic reference compounds (**6a** and **6b**), as displayed for instance by the resonances of the N-CH₂ and H₁ protons (Figure 2). Similar conclusions can be drawn from electrochemical data recorded in DCM on platinum electrodes. Each compounds exhibit two fully irreversible oxidation waves whose characteristic peak potential values are shifted upon replacing nickel with palladium ($E_{\text{pa1}}[\mathbf{6a}] < E_{\text{pa1}}[\mathbf{6b}]$). As revealed by NMR, the CV curve of the mixed compound **9** can be seen as the sum of the signatures of **6a** and **6b** with $E_{\text{pa1}}[\mathbf{9}] \approx E_{\text{pa1}}[\mathbf{6a}]$ and $E_{\text{pa2}}[\mathbf{9}] \approx E_{\text{pa1}}[\mathbf{6b}]$ (see the SI). The potential values collected for all the complexes (see SI, Table S3) can be used to provide hints about the location of electron transfer. The first oxidation potential ($E_p \sim 0.5$ V vs. SCE in all cases) collected for all the dinuclear species **6a**, **6b** and **9** is for instance consistent with a ligand-centered oxidation process. This conclusion is obviously supported by the fact that the oxidation potential is poorly influenced by the metals complexed on both sides. In addition, metal centers in most Pd(II) and Ni(II) complexes are usually not oxidized at such low potential values (Pd(III) and Ni(III) complexes are quite rare and these oxidation states are difficult to stabilize). Such preliminary analysis can unfortunately only be carried out with the first oxidation processes due to the existence of chemical steps coupled to the electron transfer (EC type of mechanism). With respect to reduction, the same reasoning can be used to attribute the waves observed at similar potential values in DMF for **6a**, **6b** and **9**. Here again the limited influence of the metal centers strongly support the conclusion that reduction occurs on the ligand rather than on the metal.

Next, we were keen to exploit the heterobimetallic nature of **9** in which the Ni center should be reactive with respect to ligand exchange reactions whereas the Pd metal should be inert. To this end, complex **9** was reacted with the unsubstituted and bischelating ligand **7** (1 molar equiv.) in THF at room temperature. After 3 days, the tetranuclear complex **10** was isolated as a dark blue powder in 46% yield. This molecule is stable in solution under air and moisture in neutral or basic conditions, but appeared sensitive to acidic medium in solution (even in CHCl₃ after several hours). Complex **10** was fully identified using NMR spectroscopy, elemental analysis and high-resolution mass spectrometry (HRMS) (see the SI). The ¹H NMR spectrum of **10** revealed the presence of signals at 5.38 (I=2), 4.72 (I=2) and 4.57 (I=4) ppm consistent with the acac C-H resonances, and with the central and external quinoidal C-H protons, respectively (see the SI). At this stage, one can infer that formation of **10** results from an associative mechanism in which the incoming ligand **7** coordinates at the Ni center and assists the dissociation of the leaving acac ligand.

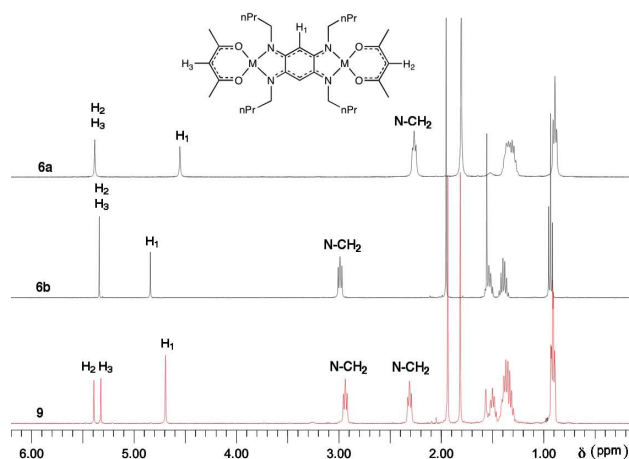


Figure 2. ^1H NMR spectra of **6a**, **6b**, and **9** in CDCl_3 .

DFT calculations have been carried out to provide further insights into the formation mechanism of **10** (see SI for details). These studies revealed that the process is not thermodynamically but kinetically controlled, and that the coordination at the nickel center of **9**, either by surrounding solvent molecules (THF) or directly by **7**, leads to the formation of a favored octahedral intermediate in which the O-Ni bond is weakened. NMR of **9** in THF-d_8 clearly indicates the absence of high spin complex (*i.e.* no coordination of solvent). We have therefore evaluated the hypothesis of a directly attacking **7** on both the Ni and Pd centers of **9** and we found that the most stable **7+9** intermediate is constituted of a high-spin octahedral Ni environment (the most stable structure is displayed in Figure 3), whereas complexation on the Pd side offers structures higher in energy irrespective of the considered spin state. Therefore, the observed reactivity is probably due to the complexation of **7**, that allows this metal to go to the more reactive triplet state, in which breaking the acac bond is easier.

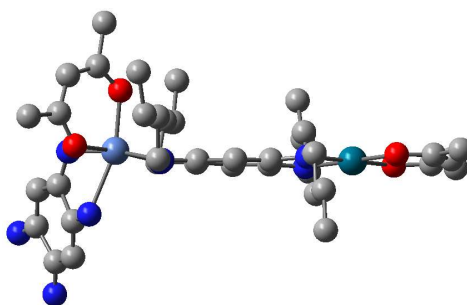


Figure 3. The most stable **7+9** intermediate that could be obtained (triplet ground-state, complexation on the Ni side). The hydrogen atoms have been omitted for clarity.

The UV-Vis absorption spectra of **8** (Pd) and **9** (Ni-Pd) exhibit broad bands centered at 421 and 445 nm for **8** and 467 and 501 nm for **9** (Figure 4). As expected, complex **10** features a pronounced redshift and the absorption extends up to the far-red region as a result of the extension of the delocalization of the conjugated π -system.¹⁴ Remarkably, a considerable hyperchromic effect is also observed ($\epsilon^{679\text{ nm}} = 110\,400\text{ M}^{-1}\text{ cm}^{-1}$ for **10** vs $\epsilon^{501\text{ nm}} = 42\,400\text{ M}^{-1}\text{ cm}^{-1}$ for **9**).

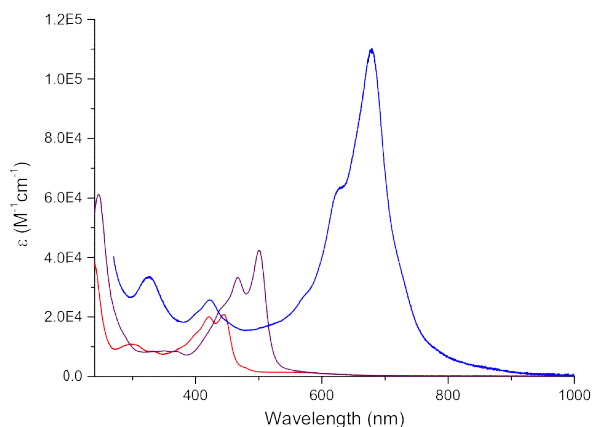


Figure 4. Absorption spectra of 8 (red), 9 (purple) and 10 (blue) in dichloromethane.

DFT calculations have also been carried out to establish relationships between the electronic spectrum and the π -electron delocalization in these compounds (see the SI for details). For **8**, **9** and **10**, TD-DFT returns the first significantly dipole-allowed excited-states at 425 nm ($f=0.34$), 423 nm ($f=1.03$) and 517 nm ($f=2.38$) respectively. Obviously, the strong hyperchromic effect when going from the smallest to the largest compound is well reproduced by theory, e.g., the oscillator strength of **10** is 2.3 times larger than the one in **9**, whereas the ratio between the measured ϵ is 2.6. The bathochromic displacement when going from **9** to **10**, is also well captured by TD-DFT (exp: -0.65 eV, theory: -0.53 eV).

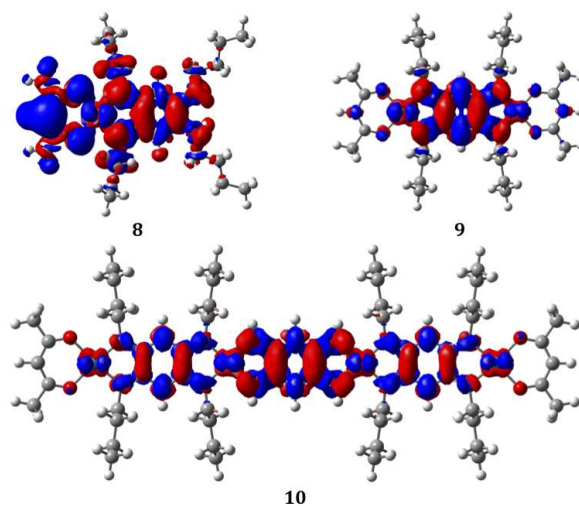


Figure 5. Density difference plots between the excited and ground states for 8, 9 and 10. Red (blue) regions indicate increase (decrease) of the density upon absorption. The selected contour threshold is 0.0004 au.

Nevertheless, we note that the computed wavelengths are too blueshifted, which is the logical consequence of neglecting vibronic effects,¹⁵ and the shift between **8** and **9** is not accurately restored by theory. The excited-states of these three compounds are analyzed as density difference plots in Figure 5. In **8**, there is a strong charge-transfer from one side (mostly in red) to the other of the molecule (mostly in blue). In contrast, the density difference plots of **9** and **10** show highly-delocalized π - π^* transitions which are strongly symmetric, involve the metallic centers, and present a nature alike the one obtained in homo-nuclear structures.¹⁴

CONCLUSION

In summary, we have reported a novel and straightforward route to access multinuclear complexes reaching the far-red region absorption. This approach is based on (i) a stepwise synthesis of a heterobinuclear Pd-Ni complex from a stable square planar mono-nuclear Pd(II) derivative, and (ii) an unprecedented heterobimetallic effect that allowed a selective concomitant ligand exchange. Soluble and stable hetero-tetranuclear complexes are now accessible for a wide range of technological sectors. As far-red -absorbing organic materials, these new dyes are highly attractive in the optoelectronic field (OPV, DSSC, photodetection, conduction).¹⁶ As multinuclear complexes, they are also relevant for catalysis,¹⁷ and selective gas sensors thanks to the presence of two different metal centers able to bind an analyte (response by spin state changes in the case of nickel for instance).¹⁸

EXPERIMENTAL SECTION

Synthesis of 6a. To a solution of ligand **2** (R = nBu) (m = 144 mg, 0.399 mmol, 1 equiv.) in THF (v = 4 mL) was added Ni(acac)₂ (m = 205 mg, 0.798 mmol, 2 equiv.). The reaction mixture was stirred at room temperature overnight and the solvent was then removed under reduced pressure. The resulting solid was taken up in Et₂O (v = 5 mL) and the obtained precipitate was isolated by filtration, washed with Et₂O (v = 3 x 10 mL) and dried under vacuum to afford **6a** as a dark green crystalline powder (m = 193 mg, 0.286 mmol, 72% yield). Monocrystal of **6a** for X-ray analysis was obtained by slow diffusion with CDCl₃ / *n*-heptane. ¹H NMR (400 MHz, CDCl₃, 294 K): δ (ppm) = 5.38 (s, 2H, CH-acac), 4.55 (s, 2H, N-C-C-H), 2.26 (t, ³J_{HH} = 7.0 Hz, 8H, N-CH₂-), 1.80 (s, 12H, CH₃-acac), 1.36-1.27 (m, 16H, -CH₂-CH₂-CH₃), 0.89 (t, ³J_{HH} = 7.0 Hz, 12H, -CH₂-CH₃). ¹³C NMR (100 MHz, CD₂Cl₂, 294 K): δ (ppm) = 187.2, 166.0, 101.6, 84.2, 43.8, 31.4, 25.8, 21.1, 14.3. HRMS (ESI-TOF): m/z [M+H]⁺ for C₃₂H₅₃N₄O₄Ni₂⁺ calcd. 673.2768, found 673.2767, err. < 1 ppm. Elemental analysis for C₃₂H₅₂N₄O₄Ni₂ (674.17): calcd. C 57.01, H 7.77, N 8.31 found C 56.94, H 7.84, N 8.18.

Synthesis of 6b. To a solution of ligand **2** (R = nBu) (m = 50 mg, 0.139 mmol, 1 equiv.) in 1,4-dioxane (v = 3 mL) was added Pd(acac)₂ (m = 85 mg, 0.279 mmol, 2 equiv.). The reaction mixture was heated overnight at 100 °C. The solvent was then removed

under reduced pressure and the resulting solid was washed with Et₂O ($v = 3 \times 3$ mL), isolated by filtration and dried under vacuum to afford **6b** as a brown crystalline powder ($m = 74$ mg, 0.096 mmol, 70% yield). Monocrystal of **6b** for X-ray analysis was obtained by slow diffusion with CDCl₃ / *n*-heptane. ¹H NMR (400 MHz, CDCl₃) δ (ppm) = 5.33 (s, 2H, *CH*-acac), 4.83 (s, 2H, *N-C-C-H*), 2.98 (t, ³*J*_{HH} = 7.2 Hz, 8H, *N-CH₂-*), 1.94 (s, 12H, *CH₃*-acac), 1.56-1.49 (m, 8H, *N-CH₂-CH₂-*), 1.43-1.34 (m, 8H, *-CH₂-CH₃*), 0.93 (t, ³*J*_{HH} = 7.3 Hz, 12H, *-CH₂-CH₃*). ¹³C NMR (400 MHz, CDCl₃) δ (ppm) = 186.3, 167.7, 101.0, 82.6, 46.8, 30.6, 26.5, 20.6, 14.1. MS (ESI-TOF): m/z [M+H]⁺ for C₃₂H₅₃N₄O₄Pd₂⁺ calcd. 771.2, found 771.2. Elemental analysis for C₃₂H₅₂N₄O₄Pd₂ (769.62): calcd. C 49.94, H 6.81, N 7.28 found C 49.89, H 6.63, N 7.13. UV-Vis Absorption in CH₂Cl₂: $\epsilon^{481\text{ nm}} = 60\,000\text{ M}^{-1}\text{cm}^{-1}$, $\epsilon^{450\text{ nm}} = 33\,200\text{ M}^{-1}\text{cm}^{-1}$, $\epsilon^{423\text{ nm}} = 15\,700\text{ M}^{-1}\text{cm}^{-1}$, $\epsilon^{338\text{ nm}} = 5\,900\text{ M}^{-1}\text{cm}^{-1}$.

Synthesis of 8. To a solution of ligand **2** ($R = n\text{Bu}$) ($m = 180$ mg, 0.499 mmol, 1 equiv.) in 1,4-dioxane ($v = 25$ mL), were added Pd(acac)₂ ($m = 152$ mg, 0.499 mmol, 1 equiv.) and aq. HBF₄ (0.153 M, $v = 3.26$ mL, 0.499 mmol, 1 equiv.). The mixture was stirred at reflux under argon for 7 h. The solvent was then removed under reduced pressure and the residue was taken up in Et₂O/CH₂Cl₂ and sonicated. The obtained precipitate was isolated by filtration, washed with Et₂O ($v = 2 \times 50$ mL) and dried under vacuum to afford **8** as a dark brown powder ($m = 284$ mg, 0.435 mmol, 81% yield). Molecule **8** is stable in solution under air and moisture. Monocrystal of **8** for X-ray analysis was obtained by slow diffusion with CH₂Cl₂ / *n*-heptane. ¹H NMR (400 MHz, CDCl₃, 294 K): $\delta = 6.86$ (br t, 2H, *NH*), 5.48 (s, 1H, *CH*-acac), 5.24 (s, 2H, *N-C-C-H*), 3.30-3.21 (m, 8H, *-CH₂-CH₂-CH₃*), 2.06 (s, 6H, *CH₃*-acac), 1.74 (quintet, ³*J*_{HH} = 7.5 Hz, 4H, *NH-CH₂-CH₂-*), 1.61 (quintet, ³*J*_{HH} = 7.5 Hz, 4H, *N-CH₂-CH₂-*), 1.48-1.37 (m, 8H, *-CH₂-CH₃*), 0.99-0.94 (m, 12H, *-CH₂-CH₃*). ¹³C NMR (100 MHz, CDCl₃, 294 K): $\delta = 186.9$, 167.5, 148.7, 101.8, 86.3, 48.4, 44.1, 31.1, 29.2, 26.3, 20.6, 20.3, 14.0, 13.7. ¹⁹F NMR (376 MHz, CDCl₃, 294 K): $\delta = -150.42$, -150.47 . HRMS (ESI-TOF): m/z M⁺ for C₂₇H₄₇N₄O₂Pd⁺ calcd. 565.2739, found 565.2740, err. < 1 ppm. Elemental analysis for C₂₇H₄₇N₄O₂Pd⁺·¹/₆CH₂Cl₂ (667.07): calcd. C 48.91, H 7.15, N 8.40; found C 48.71, H 6.66, N 8.89. UV-Vis Absorption in CH₂Cl₂: $\epsilon^{445\text{ nm}} = 20\,900\text{ M}^{-1}\text{cm}^{-1}$, $\epsilon^{421\text{ nm}} = 20\,100\text{ M}^{-1}\text{cm}^{-1}$, $\epsilon^{332\text{ nm}} = 8\,600\text{ M}^{-1}\text{cm}^{-1}$, $\epsilon^{298\text{ nm}} = 10\,900\text{ M}^{-1}\text{cm}^{-1}$.

Synthesis of 9. To a solution of **8** ($m = 50$ mg, 76.6 μmol , 1 equiv.) in MeOH ($v = 6$ mL), was added Ni(acac)₂ ($m = 62$ mg, 241 μmol , 3.15 equiv.). The reaction was stirred at 60 °C overnight. The resulting precipitate was isolated by a filtration, washed with MeOH and EtOH, dried under vacuum to afford the desired product **9** as a brown powder ($m = 20$ mg, 27.7 μmol , 37% yield). Molecule **9** is stable in solution under air and moisture. Monocrystal of **9** for X-ray analysis was obtained by slow diffusion with CH₂Cl₂ / MeOH. ¹H NMR (400 MHz, CDCl₃, 298 K): $\delta = 5.39$ (s, 1H, *CH*-acacNi), 5.32 (s, 1H, *CH*-acacPd), 4.69 (s, 2H, *N-C-C-H*), 2.94 (t, ³*J*_{HH} = 7.3 Hz, 4H, *Pd-N-CH₂-*), 2.31 (t, ³*J*_{HH} = 7.2 Hz, 4H, *Ni-N-CH₂-*), 1.94 (s, 6H, *CH₃*-acacPd), 1.81 (s, 6H, *CH₃*-acacNi), 1.54-1.46 (m, 4H, *Pd-N-CH₂-CH₂-*), 1.43-1.28 (m, 12H, *-CH₂-*), 0.93-0.89 (m, 12H, *-CH₃*). ¹³C NMR (100 MHz, CDCl₃, 294 K): $\delta = 186.5$, 186.3, 167.9, 165.5, 101.4, 100.9, 83.3, 46.8, 43.5, 31.0, 30.5, 26.5, 25.6, 20.8, 20.6, 14.1, 14.1. HRMS (ESI-TOF): m/z [M+H]⁺ for C₃₂H₅₃N₄O₄NiPd calcd. 723.2444, found 723.2445, err. < 1 ppm. Elemental analysis for C₃₂H₅₂N₄NiO₄Pd·H₂O (739.91): calcd. C 51.94, H 7.35, N 7.57; found C 52.20, H 7.12, N 7.61. UV-Vis Absorption in CH₂Cl₂: $\epsilon^{501\text{ nm}} = 42\,400\text{ M}^{-1}\text{cm}^{-1}$, $\epsilon^{467\text{ nm}} = 33\,400\text{ M}^{-1}\text{cm}^{-1}$, $\epsilon^{368\text{ nm}} = 8\,500\text{ M}^{-1}\text{cm}^{-1}$, $\epsilon^{351\text{ nm}} = 8\,700\text{ M}^{-1}\text{cm}^{-1}$, $\epsilon^{246\text{ nm}} = 61\,300\text{ M}^{-1}\text{cm}^{-1}$.

Synthesis of 10. To a solution of **9** ($m = 60$ mg, 83.1 μmol , 1.9 equiv.) in THF ($v = 5$ mL), were added **7** ($m = 5.9$ mg, 43.3 μmol , 1 equiv.) and 2 drops of *i*Pr₂NEt. The mixture was stirred at room temperature for 3 days. The resulting precipitate was isolated by a filtration and taken up in CH₂Cl₂. The insoluble solid was then filtered off and the filtrate was evaporated under vacuum to afford a crude product. This latter was washed with acetone (containing 1% Et₃N), Et₂O, and dried under vacuum to afford **10** as a dark blue powder ($m = 26$ mg, 18.8 μmol , 46% yield). ¹H NMR (400 MHz, CDCl₃, 294 K): $\delta = 5.33$ (s, 2H, *CH*-acacPd), 4.73 (s, 2H, *NH-C-C-H*), 4.71 (s, 4H, *N-C-C-H*), 3.55 (br s, 4H, *NH*), 2.95 (br t, 8H, *Pd-N-CH₂-*), 2.60 (br t, 8H, *Ni-N-CH₂-*), 1.94 (s, 12H, *CH₃*-acacPd), 1.52-1.43 (m, 8H, *Pd-N-CH₂-CH₂-*), 1.40-1.29 (m, 24H, *-CH₂-*), 0.95-0.89 (m, 24H, *-CH₃*). No ¹³C NMR spectrum of **10** could be recorded owing to its poor solubility. HRMS (ESI-TOF): m/z [M+H]⁺ for C₆₀H₉₇N₁₂O₄Ni₂Pd₂⁺, calcd. 1379.4533, found 1379.4535, error < 2 ppm. Elemental analysis for C₆₀H₉₆N₁₂O₄Pd₂·CH₂Cl₂ (1464.64): calcd. C 50.02, H 6.74, N 11.48; found C 49.60, H 6.52, N 11.93. UV-Vis Absorption in CH₂Cl₂ containing 0.5% of DIPEA: $\epsilon^{679\text{ nm}} = 110\,400\text{ M}^{-1}\text{cm}^{-1}$, $\epsilon^{628\text{ nm}} = 64\,900\text{ M}^{-1}\text{cm}^{-1}$, $\epsilon^{422\text{ nm}} = 28\,000\text{ M}^{-1}\text{cm}^{-1}$, $\epsilon^{325\text{ nm}} = 35\,500\text{ M}^{-1}\text{cm}^{-1}$.

ASSOCIATED CONTENT

¹H and ¹³C NMR spectra, theoretical calculations details, electrochemistry and mass spectrometry data. X-ray crystallographic data for **6a**, **6b** and **9**.

AUTHOR INFORMATION

Corresponding Authors

*D.J.: Denis.Jacquemin@univ-nantes.fr

*O.S.: olivier.siri@univ-amu.fr

ORCID

Christophe Bucher: 0000-0003-1803-6733

Gabriel Canard: 0000-0002-3572-9091

Michel Giorgi: 0000-0002-4367-1985

Denis Jacquemin: 0000-0002-4217-0708

ACKNOWLEDGMENT

OS acknowledges the Centre National de la Recherche Scientifique, the Ministère de la Recherche for financial support and PhD grant to ZC. OS and DJ thank the ANR for support (EMA grant). This research used resources of (1) the GENCI-CINES/IDRIS, (2) CCIPL (Centre de Calcul Intensif des Pays de Loire), (3) the local Troy cluster acquired thanks to Région des Pays de la Loire.

REFERENCES

- (1) a) Brown, E. R. *Quinonediimines, monoimines and related compounds*, in The Quinonoid Compounds (1988), John Wiley & Sons Inc, 2010, pp. 1231–1292. b) Hünig, S. Aromatic/quinoid systems: principles and applications *Pure Appl. Chem.* **1990**, *62* 395. c) Moussa, J.; Amouri, H. Supramolecular Assemblies Based on Organometallic Quinonoid Linkers: A New Class of Coordination Networks *Angew. Chem. Int. Ed.* **2008**, *47*, 1372. d) Casado, J.; Ponce Ortiz, R.; Lopez Navarrete, J. T. Quinonoid oligothiophenes: new properties behind an unconventional electronic structure *Chem. Soc. Rev.* **2012**, *41*, 5672. e) Asche, C. *Med. Chem.* **2005**, *5*, 449. f) López, J.; de la Cruz, F.; Alcaraz, Y.; Delgado, F.; Vázquez, M. A. Quinoid systems in chemistry and pharmacology *Med. Chem. Res.* **2015**, *24*, 3599. g) Ward, M. D. Metal-metal interactions in binuclear complexes exhibiting mixed valency; molecular wires and switches *Chem. Soc. Rev.* **1995**, *24*, 121. h) Demir, S.; Jeon, I.-R.; Long, J. R.; Harris, Radical ligand-containing single-molecule magnets T. D. *Coord. Chem. Rev.* **2015**, *289–290*, 149. i) Sarkar, B.; Schweinfurth, D.; Deibel, N.; Weisser, F. Functional metal complexes based on bridging “imino”-quinonoidligands *Coord. Chem. Rev.* **2015**, *293–294*, 250.
- (2) a) Masui, H.; Lever, A. B. P. Correlations between the ligand electrochemical parameter, EL(L), and the Hammett substituent parameter, σ . *Inorg. Chem.* **1993**, *32*, 2199. b) Metcalfe, R. A.; Vasconcellos, L. C. G.; Mirza, H.; Franco, D. W.; Lever, A. B. P. Synthesis and characterization of dinuclear complexes of 3,3',4,4'-tetraminobiphenyl with tetramminoruthenium and bis(bipyridine)-ruthenium residues and their two- and four-electron oxidized products including a ZINDO study of orbital mixing as a function of ligand oxidation state *J. Chem. Soc., Dalton Trans.* **1999**, 2653.
- (3) Pascal, S.; Siri O. Benzoquinonediimine ligands: Synthesis, coordination chemistry and properties *Coord. Chem. Rev.* **2017**, *350*, 178.
- (4) Kitagawa, S.; Kawata, S. Coordination compounds of 1,4-dihydroxybenzoquinone and its homologues. Structures and properties *Coord. Chem. Rev.* **2002**, *224*, 11.
- (5) a) Kimich, C. Einwirkung aromatischer Amine auf Nitrosophenol und Nitrosodimethylanilin *Chem. Ber.* **1875**, *8*, 1026. b) Fischer, O.; Hepp, E. Ueber Azophenin und Chinonanilide. II *Chem. Ber.* **1888**, *21*, 676. c) Bandrowski, E.V. Über die Oxydation des Paraphenylendiamins und des Paraamidophenols *Monatsh. Chem.* **1889**, *10*, 123. d) Siri, O.; Braunstein, P. First binuclear complex of an N,N',N'',N'''-tetraalkyl 2,5-diamino-1,4-benzoquinonediimine *Chem. Commun.* **2000**, 2223. e) Siri, O.; Braunstein, P.; Rohmer, M.-M.; Bénard, M.; Welter, R. Novel “Potentially Antiaromatic”, Acidichromic Quinonediimines with Tunable Delocalization of Their σ -Electron Subunits *J. Am. Chem. Soc.* **2003**, *125* 13793. f) Seillan, C.; Braunstein, P.; Siri, O. Selective Reduction of Carbonyl Amides: Toward the First Unsymmetrical Bischelating N-Substituted 1,2-Diamino-4,5-di-amidobenzene *Eur. J. Org. Chem.* **2008**, 3113. g) Wenderski, T.; Light, K. M.; Ogrin, D.; Bott, S. G.; Harlan, C. J. Pd catalyzed coupling of 1,2-dibromoarenes and anilines: formation of N,N-diaryl-o-phenylenediamines *Tetrahedron Lett.* **2004**, *45*, 6851. h) Khranov, D. M.; Boydston, A. J.; Bielawski, C. W. Highly Efficient Synthesis and Solid-State Characterization of 1,2,4,5-Tetrakis(alkyl- and arylamino)benzenes and Cyclization to Their Respective Benzobis(imidazolium) Salts *Org. Lett.* **2006**, *8*, 1831. i) Ohno, K.; Nagasawa, A.; Fujihara, T. Dinuclear nickel(II) complexes with 2,5-diamino-1,4-benzoquinonediimine ligands as precatalysts for the polymerization of styrene: electronic and steric substituent effects *Dalton Trans.* **2015**, *44*, 368. j) Abdelhameed, M.; Langlois, A.; Fortin, D.; Karsenti, P.-L.; Harvey, P. D. A drastic substituent effect on the emission properties of quinone diimine models and valuable insight into the excited states of emeraldine *Chem. Commun.* **2014**, *50*, 11214. k) Andeme Edzang, J.; Chen, Z.; Audi, H.; Canard, G.; Siri, O. Transamination at the Crossroad of the One-Pot Synthesis of N-Substituted Quinonediimines and C-Substituted Benzobisimidazoles *Org. Lett.* **2016**, *18*, 5340.
- (6) a) Rall, J.; Stange, A. F.; Hübler, K.; Kaim, W. A Coordination-Induced 1,4→1,2-Quinonediimine Isomerization *Angew. Chem. Int. Ed.* **1998**, *37*, 2681. b) Frantz, S.; Rall, J.; Hartenbach, I.; Schleid, T.; Zálaiš, S.; Kaim, Metal-Induced Tautomerization of p- to o-Quinone Compounds: Experimental Evidence from CuI and ReI Complexes of Azophenine and DFT Studies *Chem. Eur. J.* **2004**, *10*, 149. c) Braunstein, P.; Demessence, A.; Siri, O.; Taquet, J.-P. Relocalisation of the π system in benzoquinonediimines induced by metal coordination *C. R. Chim.* **2004**, *7*, 909.
- (7) a) Cheng, H.-Y.; Lee, G.-H.; Peng, S.-M. Coordination chemistry of sulfonyl amides 3. Copper(I) and nickel(II) complexes of N, N',N'',N'''-tetramethylsulfonyl-1,4-benzoquinonediimine-2,5-diaminato *Inorg. Chim. Acta* **1992**, *191*, 25–27. b) Trumm, C.; Hübner, O.; Kaifer, E.; Himmel, H.-J. Trapped in a Complex: the 1,2,4,5-Tetrakis(tetramethylguanidino)benzene Radical Cation (ttmgb⁺) with a Bisallylic Structure *Eur. J. Inorg. Chem.* **2010**, 3102. c) Jeon, I.-R.; Park, J. G.; Xiao, D. J.; Harris, T. D. An Azophenine Radical-Bridged Fe₂ Single-Molecule Magnet with Record Magnetic Exchange Coupling *J. Am. Chem. Soc.* **2013**, *135*, 16845. d) DeGayner, J. A.; Jeon, I.-R.; Harris, T. D. A series of tetraazalene radical-bridged M₂ (M = Cr^{III}, Mn^{II}, Fe^{II}, Co^{II}) complexes with strong magnetic exchange coupling *Chem. Sci.* **2015**, *6*, 6639.
- (8) a) Taquet, J.-P.; Siri, O.; Braunstein, P.; Welter, R. Dinuclear Nickel and Palladium Complexes with Bridging 2,5-Diamino-1,4-benzoquinonediimines: Synthesis, Structures, and Catalytic Oligomerization of Ethylene *Inorg. Chem.* **2006**, *45*, 4668. b) Huang, Y.-B.; Tang, G.-R.; Jin, G.-Y.; Jin, G.-X. Novel, Highly Active Binuclear 2,5-Disubstituted Amino-p-benzoquinone–Nickel(II) Ethylene Polymerization Catalysts *Organometallics* **2008**, *27*, 259. c) Siri, O.; Taquet, J.-p.; Braunstein, P.; Collin, J.-P.; Rohmer M.-M.; Bénard, M. Tunable Charge Delocalization in Dinickel Quinonoid Complexes *Chem. Eur. J.* **2005**, *11*, 7247.
- (9) Su, Y.; Zhao, Y.; Gao, J.; Dong, Q.; Wu, B.; Yang, X.-J. Alkali Metal and Zinc Complexes of a Bridging 2,5-Diamino-1,4-Benzoquinonediimine Ligand *Inorg. Chem.* **2012**, *51*, 5889.
- (10) a) Schweinfurth, D.; Khusniyarov, M. M.; Bubrin, D.; Hohloch, S.; Su, C.-Y.; Sarkar, B. Tuning Spin–Spin Coupling in Quinonoid-Bridged Dicopper(II) Complexes through Rational Bridge Variation *Inorg. Chem.* **2013**, *52*, 10332. b) Deibel, N.; Sommer, M. G.; Hohloch, S.; Schwann, J.; Schweinfurth, D.; Ehret, F.; Sarkar, B. Dinuclear Quinonoid-Bridged d₈ Metal Complexes with Redox-Active Azobenzene Stoppers: Electrochemical Properties and Electrochromic Behavior *Organometallics* **2014**, *33*, 4756.
- (11) Ohno, K.; Fujihara, T.; Nagasawa, A. Formation of boron, nickel(II) and iridium(III) complexes with an azophenine derivative: Isomerization, delocalization and extension of the π -conjugated system on coordination *Polyhedron* **2014**, *33*, 715.
- (12) a) Basolo, F.; Pearson, R. G. *Mechanisms of Inorganic Chemistry*, 2nd edn, Wiley, New York, 1967; b) Wilkins, R. G. *The Study of Kinetics and Mechanism of Reactions of Transition Metal Complexes*, Allyn Bacon, Boston 1974 chapt.7.
- (13) a) Porterfield, W. W. *Inorganic Chemistry*, Addison-Wesley, Reading, MA, 1983, pp. 561–575; b) Langford, C. H.; Gray, H. B. *Ligand Substitution Processes*, W.A. Benjamin, New York, 1966; c) Jordan, R. B. *Reaction Mechanisms of Inorganic and Organometallic Systems*, 2nd

edn, Oxford University Press, New York, 1998, p. 116; d) Sykes, A. G. *Kinetics of Inorganic Reactions*, Pergamon Press, New York, 1966, pp. 250–261.

(14) Audi, H.; Chen, Z.; Charaf-Eddin, A.; D'Aleo, A.; Canard, G.; Jacquemin, D.; Siri, O. Extendable nickel complex tapes that reach NIR absorptions *Chem. Commun.* **2014**, *50*, 15140.

(15) Santoro, S. ; Jacquemin D. Going beyond the vertical approximation with time-dependent density functional theory *WIREs Comput Mol Sci* **2016**, *6*, 460.

(16) Qian, G. ; Wang, Z. Y. Near-Infrared Organic Compounds and Emerging Applications *Chem. – Asian J.* **2010**, *5*, 1006.

(17) a) Moriuchi, T.; Hirao, T. *Design and Redox Function of Conjugated Complexes with Polyanilines or Quinonediimines* *Acc. Chem. Res.* **2012**, *45*, 347. b) Ishii, Y.; Sakaguchi, S.; Iwahama, T. Innovation of Hydrocarbon Oxidation with Molecular Oxygen and Related Reactions *Adv. Synth. Catal.* **2001**, *343*, 393. c) Ward M. D.; McCleverty, J. A. Non-innocent behaviour in mononuclear and polynuclear complexes: consequences for redox and electronic spectroscopic properties *J. Chem. Soc., Dalton Trans.*, **2002**, 275. d) Bäckvall, J.-E. *Modern Oxidation Methods*, Wiley-VCH, Weinheim, Germany, 2004. e) Holliday B. J.; Swager, T. M. Conducting metallopolymers: the roles of molecular architecture and redox matching *Chem. Commun.* **2005**, 23. f) Nishihara, H. Combination of redox- and photochemistry of azo-conjugated metal complexes *Coord. Chem. Rev.*, **2005**, *249*, 1468. g) Wolf, M. O. Recent Advances in Conjugated Transition Metal-containing Polymers and Materials *J. Inorg. Organomet. Polym. Mater.*, **2006**, *16*, 189.

(18) Kar, P.; Yoshida, M.; Shigeta, Y.; Usui, A.; Kobayashi, A.; Minamidate, T.; Matsunaga, N.; Kato, M. Methanol-Triggered Vapochromism Coupled with Solid-State Spin Switching in a Nickel(II)-Quinonoid Complex *Angew. Chem. Int. Ed.* **2017**, *56*, 2345.